Metallurgical and Materials Engineering *Research paper*
Association of Metallurgical Engineers of Serbia AMES *https://doi.org/10.30544/858*

SYNTHESIS AND CHARACTERIZATION OF BIOCOMPOSITES BASED POLYPROPYLENE/THERMOPLASTIC STARCH-REINFORCED WITH NATURAL *STIPA TENACISSIMA* FIBERS AND PP-g-MA

A. *S. Chabira* [*], C. Bouremel, A. Sakri, A. Boutarfaia

Laboratory of Applied Chemistry, University of Biskra, BP 145 RP, 07000 Biskra, Algeria

Received 29.06.2022

Accepted 09.08.2022

Abstract

The current work aims to develop environmentally friendly plastic materials by preparing a composite polypropylene/thermoplastic starch (PP/TPS) using a melt-compounding process. In order to improve the compatibility of the two naturally incompatible polymers, natural Stipa tenacissima fibers treated on their surfaces and polypropylene (PP) pellets grafted with Maleic Anhydride (MA) were added to the mixture (PP and TPS). The mixture was then prepared using the melt-mixing method in various concentrations. X-ray diffraction (XRD), scanning electron microscopy (SEM), thermogravimetric analysis (TGA)/Differential thermal analysis (DTA), and mechanical tensile tests were then used to characterize the various formulations. SEM images revealed that the addition of (PP-g-MA) and natural fibers resulted in good starch plasticization and higher thermoplastic starch dispersion in the polypropylene matrix. It was also discovered that increasing the TPS concentration over the PP concentration tends to reduce the mechanical tensile properties. However, the composite with 15% TPS had the best mechanical properties. The thermogravimetric analysis (TGA) results revealed that the organic filler used acted as a reinforcing agent, increasing the thermal stability of the polypropylene/thermoplastic starch (PP/TPS) compound.

Keywords: thermoplastic starch; organic filler; polypropylene; PP-g-MA.

[*] Corresponding author: *Chabira Amel Samia, samia.chabira@univ-biskra.dz*

Introduction

Due to the strict legal environmental requirements and regulations concerning the disposal of polymers once they become waste after use, biodegradable materials have attracted the attention of a large number of researchers in recent years [1]. Corn starch has been widely reported to be one of the most biodegradable materials that can be used in a wide range of industrial and commercial applications [2-7]. No one can deny that the ever-increasing environmental issues of sustainability and ecology have been the primary motivators for the development of bio-based biodegradable plastics. It is worth noting that biodegradability is highly advantageous in single-use packaging applications, while poor mechanical properties are acceptable. On the other hand, the automotive industry has become much more difficult in recent years because durable bioplastics are expected to meet extremely demanding constraints such as high thermo-mechanical performance (strength and rigidity), as well as dimensional accuracy and stability [8-10]. Thermoplastic starch (TPS) has been identified as one of the most promising biodegradable polymers [11]. Starch is a biopolymer that is renewable, inexpensive, and abundant. Because of its hygroscopic nature, TPS can be obtained by plasticizing starch and typically blending it with another hydrophobic polymer, according to several authors [12-19]. TPS was discovered to be completely biodegradable in soil and water. TPS, on the other hand, has significant drawbacks such as poor mechanical properties and hydrophilicity. TPS can be blended with synthetic polymers such as polypropylene (PP), which is highly hydrophobic and has superior mechanical properties, to overcome these drawbacks. In general, TPS cannot guarantee the physical-chemical and mechanical properties required for a given application, such as a fossil-origin plastic. To compensate for this shortcoming, it is frequently mixed with a polyolefin to which vegetable or mineral fillers can be added to strengthen its properties [18, 20]. The main benefit of combining a biopolymer and a synthetic polymer is that the proportion of non-biodegradable plastic material is reduced. While we wait for the ability to produce 100% biodegradable polymers, this approach is a first step toward reducing the amount of non-biodegradable materials dumped in nature. This is why many efforts are made to discover biodegradable and renewable polymers, such as starch-based biopolymers, that can help to preserve nature. It should be noted that polypropylene (PP) could be a suitable polymer to mix with TPS due to its appealing properties such as low weight, low density, and low cost, in addition to its melting temperature of approximately 160 ° C. Although its melting temperature is slightly higher than TPS's, it is not so high that it will degrade during processing [18-22].

Furthermore, polypropylene and thermoplastic starch were found to be highly immiscible. Several approaches have been tried in the past to improve the miscibility of the polypropylene (PP) matrix phase and the thermoplastic starch (TPS) phase. Some of these approaches include using starch derivatives such as starch phthalate [23] and commercial starch-based blends such as Mater-Bi type bioplastic to improve miscibility [24].

However, reactive polymer extrusion and the addition of a compatibilizer, such as polypropylene-grafted-maleic anhydride (PP-g-MA), can significantly reduce interfacial tension between two immiscible phases. The esterification reaction between the polypropylene-grafted-maleic anhydride (PP-g-MA) copolymer and the starch hydroxyl groups is widely acknowledged to be used to improve the compatibility between the two phases [8].

The objective of this study was the preparation of biodegradable composites with suitable properties. To accomplish this, corn starch was plasticized with distilled water and glycerol. The thermoplastic starch was then mixed with polypropylene in various ratios and with varying amounts of PP-g-MA. The fibers from *Stipa tenacissima* were then alkaline treated before being used as organic fillers in composites. Mechanical tensile tests and thermal analysis (TGA/DTA) were performed to compare the properties of the various formulations. Fourier transform infrared spectroscopy (FTIR) and X-ray diffraction (XRD) were also used to highlight the effect of the different constituent concentrations on the microstructure of the composites. Scanning electron microscopy was used to examine the morphology and surface topology of the various composites (SEM).

Experimental

Materials

Polypropylene (PP) HD168MO supplied by Abu Dhabi Polymers Co. Ltd (Borouge) in UAE was used. Its melting point extends from (130 to 170 °C), with a density of 0.91 g/cm^3. The melt flow rate (MFR) of this material in less than (7g/10 minutes at 230°C/2.16 kg). This polymer was then modified with maleic anhydride (MAH, 0.6 Wt. %, Aldrich). The starch used is a native corn starch marketed by Sigma-Aldrich; the amyloidosis and amylopectin levels were (23% and 77%), respectively. The density of the glycerol used is (1.25g/ml) at 25°C. The organic filler used is the *Stipa tenacissima* (natural fibers) harvested from the region of M'sila (Algeria).

Filler preparation

The first step was to thoroughly clean the *Alfa* fiber (*Stipa tenacissima*) stems with cold water. For four days, these stems were air-dried before being cut into small pieces and ground. Following that, the fibers were washed and extracted by placing them in a container with a specific amount of ethanol. The next step was to wash them with distilled water and dry them in an oven at 40° C for 48 hours. The finished product was then screened through various sieves (the mesh size of the sieve used in this work is 180 μm). It should be noted that the *Alfa* fibers obtained were treated with a natural alkali solution on their surfaces. To perform the treatment, the fibers were first immersed in a solution (1% NaOH) at (30°C) for 15 minutes (24 h). They were then washed several times with distilled water to remove the NaOH residues that remained on the fibers' surface. Any traces of NaOH were neutralized by immersing the obtained filler (*Stipa tenacissima* fibers) for 10 minutes in a (2% sulfuric acid solution). They were then washed with distilled water again until they reached a neutral solution (pH = 7). Finally, the fibers were drained at room temperature for (24 hours) before being oven-dried at (80°C, for 24 hours).

Preparation of polypropylene/thermoplastic starch/filler blends

The thermoplastic starch (TPS) was created by mixing native corn starch (65% wt.%), glycerol (25 wt.%), and water (10 wt.%) for 48 hours. After that, everything is placed in a plastic bag for 24 hours to allow the water and glycerol to penetrate the starch. The plastic bag was chosen because it can prevent either water or glycerol from evaporating into the atmosphere, thereby preventing a change in their respective initial concentrations. The polypropylene was then added. It is still possible to see that 3% PP-

g-MA and 3% alkaline fibers (*Stipa tenacissima*) were added to each formulation. Table 1 shows the concentrations of the constituents of each composite (TPS/PP/PP-g-MA/filler). A twin-screw extruder (HAAKE PolyLab QC) was used to perform the processing and homogenize the segregation of the different constituents in the composite.

Table 1. Concentration in % of the different constituents of the 6 composites (S1-S6) made of (TPS/PP/PP-g-MA/filler).

Samples	TPS (%)	PP-g-MA (%)	PP (%)	Organic Filler (%)
S1	0	3	94	3
S2	5	3	89	3
S3	10	3	84	3
S4	15	3	79	3
S5	20	3	74	3
S6	25	3	69	3

The temperature of the three heating zones was respectively 150 °C for the feed zone, 160 °C for the compression zone and finally 170 °C for the metering zone. The rods exiting from the machine were then crushed using a plastic crusher machine. The last operation consisted in molding thin plate at 170 °C by means of a hydraulic press.

Characterization

Mechanical characterization

The tensile test machine used for the mechanical testing was MTS 45 criterion (MTS Systems Corp., USA) equipped with a force cell of 5 KN. The cross-head speed was fixed to 1mm/min. The test pieces were cut from the plate according to the ISO 527-1 standard. The tests were run at room temperature (≈ 20 °C).

Microscopy

Scanning electron microscopy (SEM) was carried out to analyze the composites morphology. SEM analysis was performed using a Thermo Scientific Quattro Environmental Scanning Electron Microscope (SEM, Thermo fisher scientific, USA). The electron acceleration voltage was fixed at 20 kV.

FTIR

A Spectrum Two ATR, FTIR spectrometer, maintained by PerkinElmer (USA), was used for the infrared analysis. The infrared spectra were collected in the transmission mode over the wavenumbers range [4000-400 cm^{-1}] at a 4 cm^{-1} optical resolution and using 32 scan repetitions.

The assignment of the vibrational bands belonging to the chemical structures constituting the material was carried out based on the spectra delivered by the equipment.

Measurements by X-ray diffraction analysis

XRD measurements were conducted with an Empyrean XRD system (France) diffractometer at atmospheric pressure and room temperature. The apparatus is equipped with a copper anode and the $K_{\alpha 1}$ rays having a wavelength of 0.154 nm were selected. The diffractometer was operated at 40 kV and 40 mA.

Thermogravimetric/Differential thermal analyses (TGA/DTA)

The thermogravimetric/differential thermal (TGA/DTA) analyses of the bio-composites were conducted on a thermogravimetric analyzer (Setaram Labsys Evo, Caluire, France). The samples weight varied from (20 to 30 mg). Samples were heated from room temperature up to (600°C) with a heating rate of (10°C/min).

Results and discussion

SEM images of *Alfa* (*Stipa tenacissima*) fibers before and after treatment are shown in Fig.1. The presence of some protuberances can still be seen on the surface of the untreated fiber, as shown in Fig.1a. These last ones vanished after the chemical treatment, revealing pores instead of protuberances, as shown in Fig.1b. This is almost certainly due to the leaching of all waxy and fatty substances from the surface of the fiber. Indeed, *Rokbi et al.* [25] and *Ajouguim et al.* [26] reported that the chemical treatment removes some amorphous materials such as wax, pectin, and hemicellulose, which tends to increase the specific surface of the fibers and thus the surface contact with the matrix.

As a result, the morphology of the composite with treated or untreated fibers is expected to affect the surface aspect of the material. To demonstrate this effect, SEM images of native corn starch Fig.2a, TPS without filler Fig.2b, and TPS with treated filler Fig.2c are shown in Fig.2.

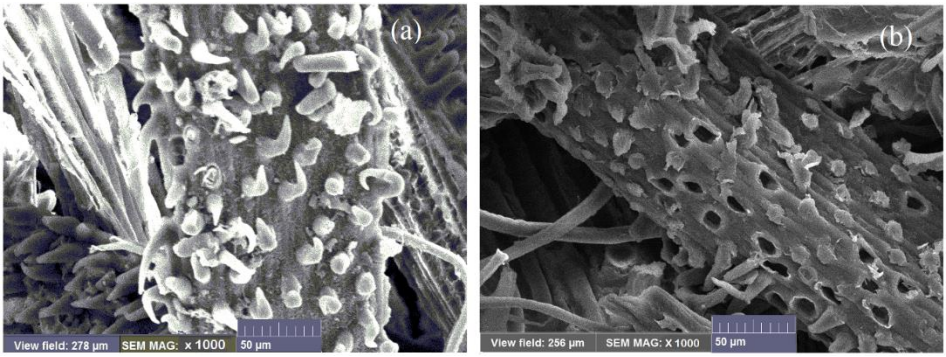

Fig. 1. SEM images of the Alfa (a) before treatment (b) after treatment.

Before processing, the different sizes of corn starch granules were easily distinguished (Fig.2a). However, after being processed into a film, the surface became a continuous phase with only a few residual unmelted polymer granules (Fig.2b). Despite this, the addition of *Alfa* fibers improved the topology of the film surface, making it appear monophasic and more regular, with almost no unmelted granules remaining (Fig.2c). As a result, the addition of organic fillers to a biopolymer improves the adhesion between the TPS units, resulting in a more regular surface.

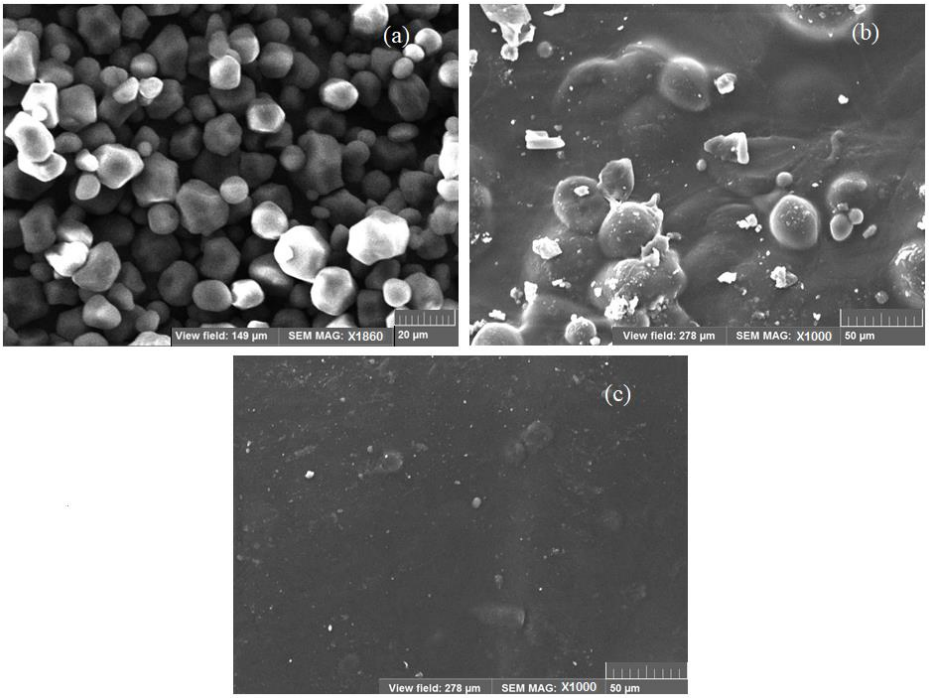

Fig. 2. SEM images of the: (a) native corn starch before processing, (b) TPS without filler, (c) TPS with treated filler.

SEM images of six different formulations are shown in Fig. 3. The concentration of the various constituents has a significant impact on the surface aspect of the films. The surface of the composite S1, which is made only of PP and filler and is free of TPS, is the most regular and continuous.

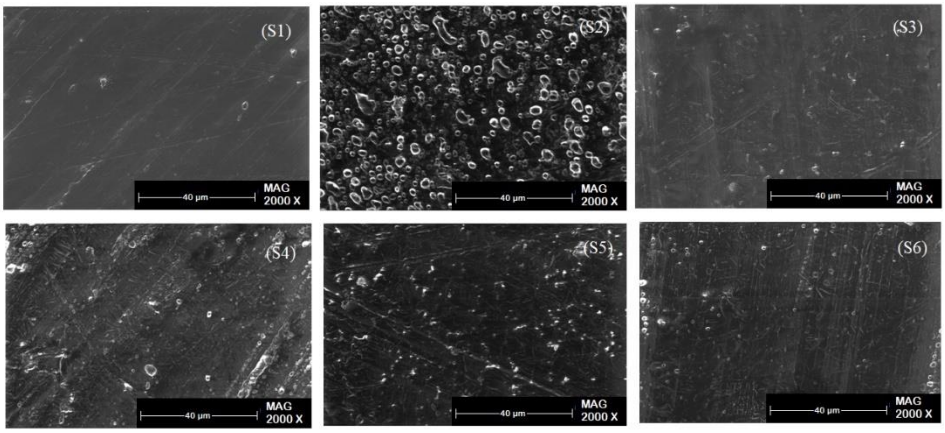

Fig. 3. SEM Images of the surface of 6 formulations (S1-S6), Mgnification X1000.

The (PP/filler) mixture without TPS has a continuous morphology. The filler (3 Wt.%) in the mixture is uniformly mixed and distributed throughout the polypropylene matrix, resulting in a homogeneous phase [27]. The use of a compatibilizer (3% PP-g-MA) and the small size of the filler both contributed to a better distribution of the fillers in the composite. Indeed, *Bajwa et al.* [27] discovered that when the composite's components are extruded under proper conditions, the fillers are continuously and uniformly mixed throughout the PP matrix, and the use of the compatibilizer greatly contributes to the formation of a homogeneous phase. This finding supports the hypothesis that maleic anhydride promotes strong ester bonds between the PP chains and the fiber's O-H groups. Otherwise, the S2 formulation has a more irregular surface and poor dispersion of the two phases. It appears that the 5% TPS added to PP is insufficient to achieve good miscibility between the two polymers. What appears to be droplets are most likely gelatinized starch granules distributed irregularly throughout the PP matrix. Indeed, as the concentration of TPS in the other formulations increases, the surface becomes more and more regular, becoming (S6) almost as regular as that of PP alone (S1). Others have shown that mixing TPS with polyolefin can result in a co-continuous morphology, but adding a polyolefin grafted with maleic anhydride can result in a more homogeneous phase [23, 27, 28].

Fourier Transform Infra-Red Spectroscopy

The FTIR spectrum of the TPS film is shown in Fig.4. It demonstrates absorption bands associated with the functional groups of corn starch and glycerol. On the FTIR spectrum, these large absorption bands appear at 920, 1022, and 1146 cm^{-1} (CO stretching), 1648 cm^{-1} (bound water), 3277 cm^{-1} (OH groups), 2920 cm^{-1} (CH stretching), 3250 cm^{-1} (large bonding of O-H groups), and 1423 cm^{-1} (glycerol). These findings are consistent with those of other authors [29].

Fig.5 shows the spectra of six formulations of (PP/PP-MA) and (PP/PP-MA/TPS/filler). The presence of (PP-MA) was indicated by peaks at 1647 cm^{-1} and 1738 cm^{-1}, which corresponded to the stretching vibrations of the C = O group. Similarly, the peak at 1163 cm-1 in the cyclic maleic anhydride shows symmetric carbonyl stretching (C - O - C group), in addition to the peak at 815 cm^{-1} that corresponds to the C = C group. All of these absorption peaks are typical of maleic anhydride (MA).

Based on these findings, it is possible to conclude that pp-g-MA was grafted onto the PP matrix [27, 30]. *Raee et al.* [19] demonstrated that the grafted maleic anhydride functional group (PP-g-MA) forms covalent bonds with the hydrophilic starch, making it the most acceptable and cost-effective compatibilizer for PP/TPS blends. Furthermore, the spectra of S2, S3, S4, S5, and S6 explicitly show the blend's characteristic peaks (PP/TPS/PP-MA/filler). In fact, the peak at 1023 cm-1 corresponds to the hydrogen bonding that connects starch to plasticizers. Furthermore, the adsorption bands between 1000 cm-1 and 1500 cm-1 are attributed to the stretching of the -C-O bond of the -C-O- H group. The presence of O-H groups in the broad transmission band between 3000 cm-1 and 3403 cm-1, on the other hand, confirms that the filler underwent a good superficial treatment due to the O-H groups associated with the hydrogen bonds [31, 32].

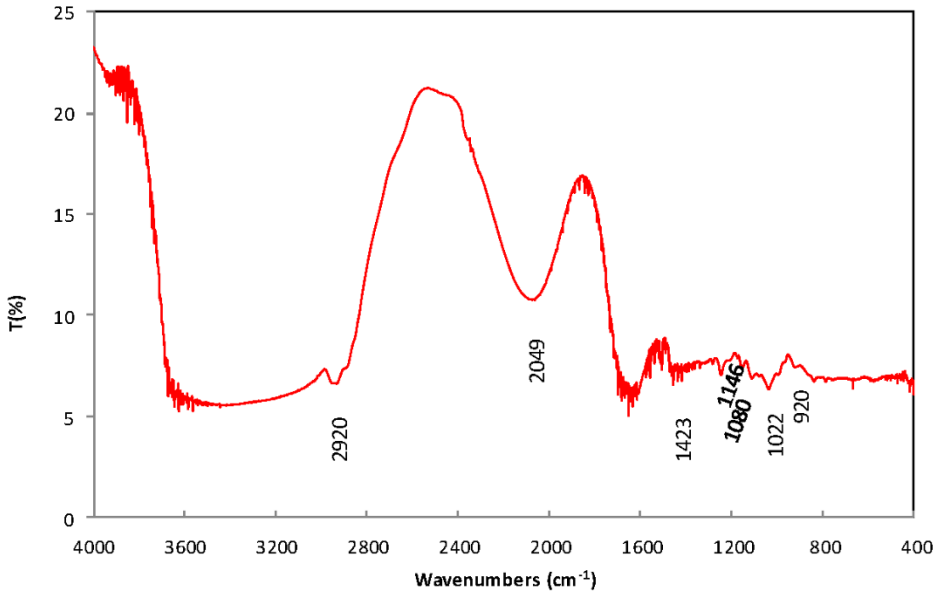

Fig. 4. IR spectrum of the TPS film

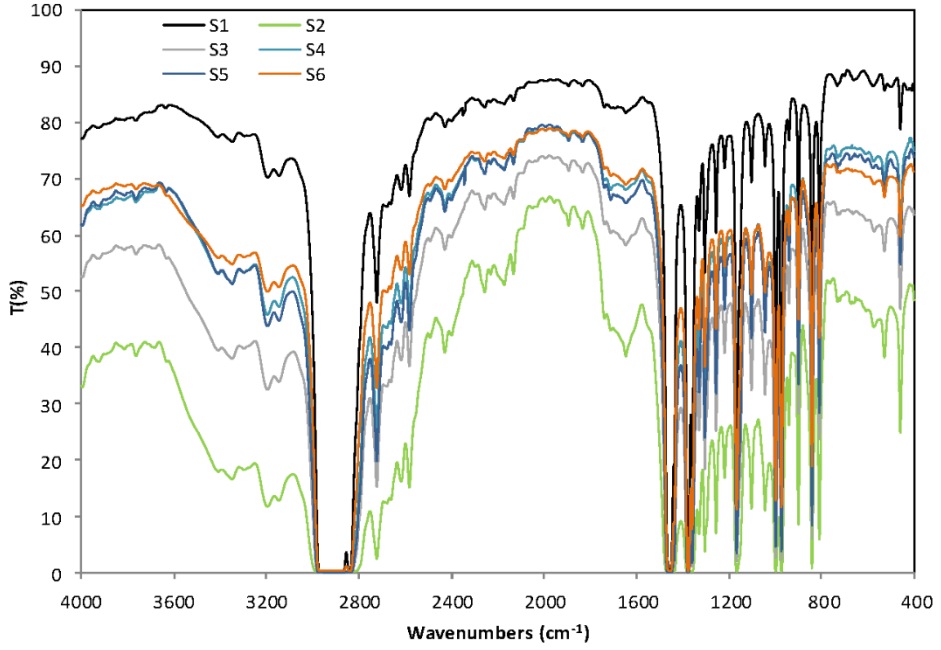

Fig. 5. FTIR spectra of 6 formulations of PP, and PP/TPS /PP-g-MA/Filler.

X-ray diffraction

Figure 6 shows the composites' X-ray diffraction patterns. TPS films exhibited diffraction peaks and a broad amorphous halo, which is typical of a semi-crystalline polymer with low crystallinity [29]. It revealed two TPS-specific peaks at 2=14.7251° and 22.5056°, respectively [33]. While sharp peaks appeared at 2 = 13.9670°, 16.7169°, 19.9014°, 21.7443°, 25.2872°, 28.5602°, and 42.3334° for the composite made entirely of PP (S1), these correspond to the crystallographic planes (110), (040), (130), (111), (041), (060), (220), and (220). These peaks are shared by all PP-containing composites. The concentration of PP and/or TPS had an effect on the appearance of the diffraction patterns and the intensity of the peaks. However, the addition of TPS changes the intensity of the peaks corresponding to the crystallographic planes of PP rather than their position.

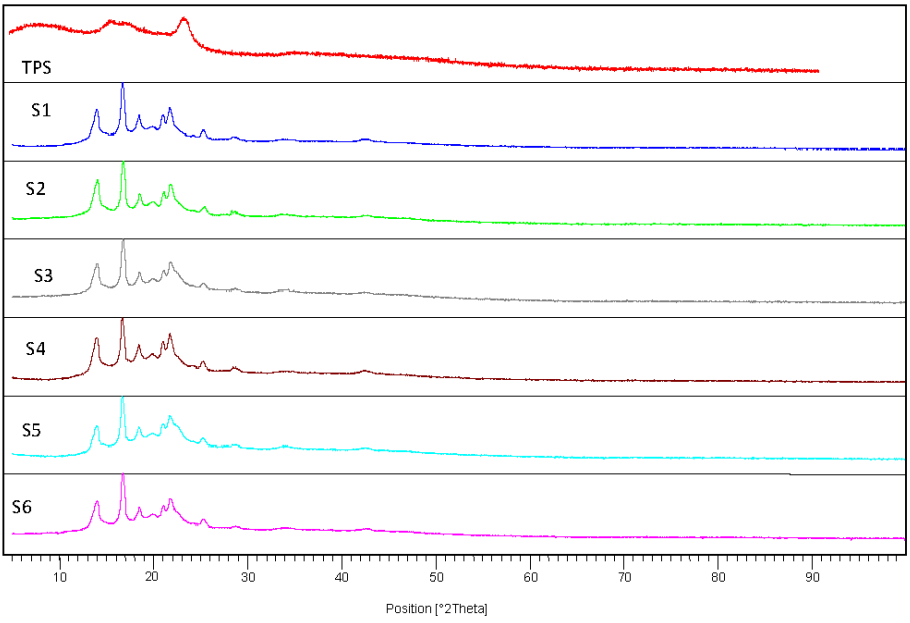

Fig. 6. X-ray Diffractograms of PP, TPS and PP/PP-AM/TPS/filler composites.

Mechanical properties

Figure 7 depicts the stress-strain curves of the PP/TPS composites (S1, S2, S3, S4, S5, and S6). It can be seen that increasing the TPS concentration gradually leads to a decrease in the properties at break [32] as well as the stiffness. Indeed, the representation of the ultimate properties (i.e.σ_r and ε_r) and the Young's modulus as a function of TPS concentration (Fig. 8) clearly shows that they decrease as TPS concentration increases. For example, in (Fig. 8a), the tensile strength decreases from 38.2 MPa for pure PP to 13.5 MPa for the composite formulated with 25 Wt.% TPS, representing a reduction of approximately 35, 34%.

The same thing can be seen for the elongation at break, which drops from 13.4 to 6.7 Mpa, a 50% decrease that is even more significant than the stress at break.

This appears to indicate that there is a weak cohesion between these two components in the various composites due to their poor compatibility.

It is important to remember that polypropylene is hydrophobic, whereas TPS is highly hydrophilic. As a result, the presence of TPS in the PP matrix tends to agglomerate, resulting in stress concentration zones and weak points in the bulk, lowering the ultimate mechanical properties. A cursory examination of the various graphics (Fig. 8 a, b, c) reveals that sample S4 made with 15% TPS has better mechanical properties than the other composites. This last one appears to be an exception, implying that the miscibility of PP and TPS for this particular concentration of TPS is very likely the best. As a consequence, it is possible to conclude that the addition of 15% TPS to the polypropylene matrix is the appropriate concentration capable of increasing the properties at break as well as the stiffness when compared to the other samples (S2, S3, S5, and S6).

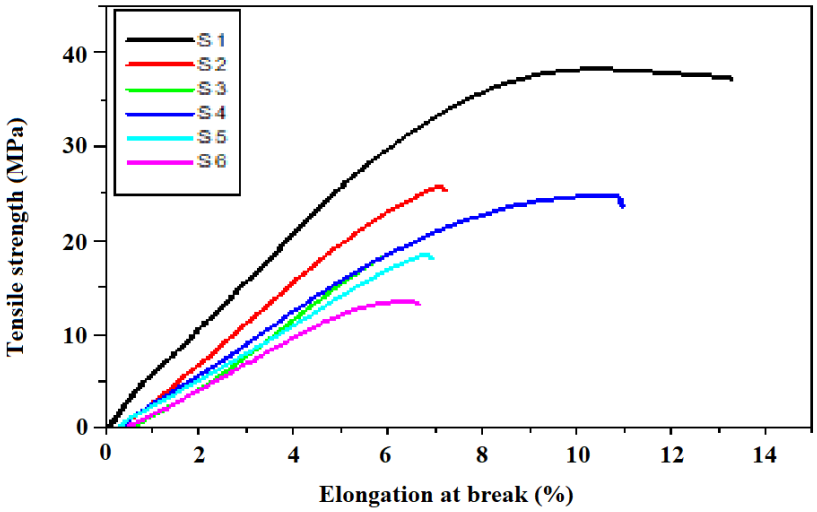

Fig. 7. Stress-strain curves of the 6 different formulations.

This result is in good agreement with other authors who reported that in some cases the Young's modulus can be increased with the addition of TPS and this is due to the stiffening effect of the starch granules [19, 32, 34].

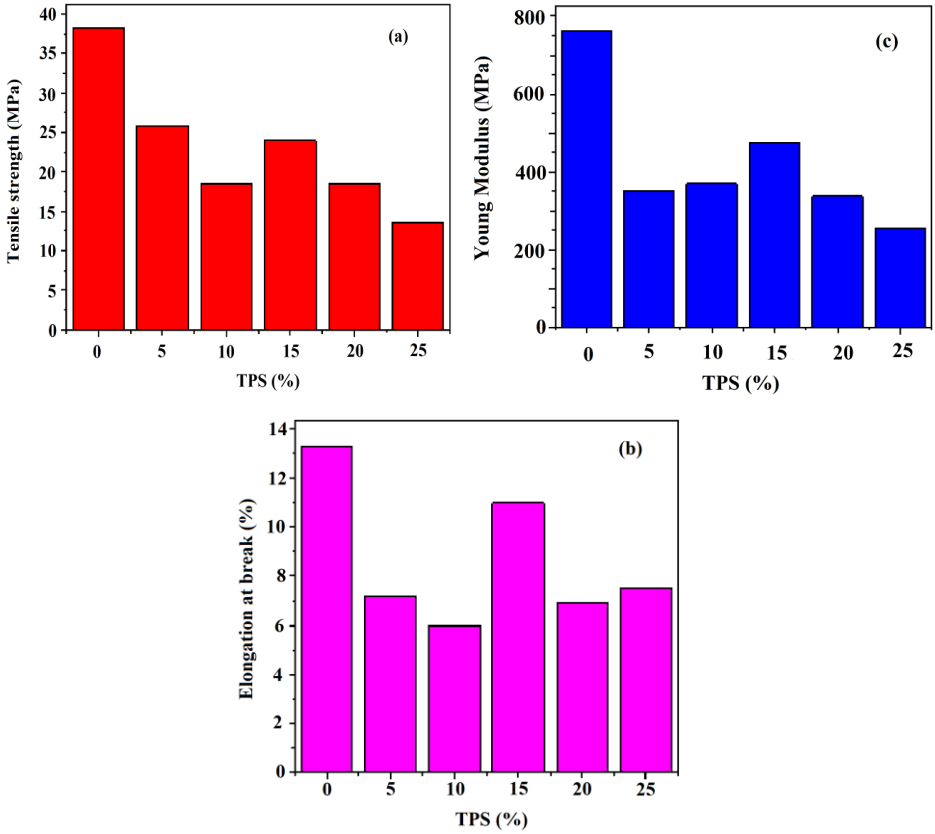

Fig. 8. (a) Tensile strength, (b) Elongation at break (%) and (c) Young's modulus as function of the TPS concentration.

Thermogravimetric analysis

Each polymer has its own thermal behavior; however, the addition of one to the other affects such behavior without a doubt. Thermal analyses using TGA and DTA were performed on the TPS alone and on the various composites to determine the effect of increasing TPS concentration on PP's thermal properties (S1-S6). The (TGA and DTA) curves of six formulations tested at temperatures ranging from 50 to 650 °C are shown in Figs. 6a and 6b. The TGA curve of TPS clearly shows that weight loss occurs from the start of the experiment, although at a slow rate. However, around 220 °C, the rate abruptly accelerates to 300 °C. The sample weight decreases by 75% between these two temperatures. The rate of weight loss slows dramatically from 300 °C to 650 °C, with an overall weight loss of only 5% in this temperature range. TPS's weight loss occurs much earlier than that of the other composites. According to the authors, the first zone of the TGA curve of the TPS corresponds primarily to water volatilization. The abrupt decrease then corresponds to plasticizer decomposition, followed by starch decomposition, and the final plateau is characteristic of residue carbonization [19].

The presence of PP in the composites delays the onset of weight loss significantly. Indeed, for PP alone, the weight loss begins well above 350 °C and is followed by an abrupt drop in the TG curve's base line. It stabilizes around 450 °C and is followed by a plateau where no more matter is released. This corresponds to the total carbonization of the residue found at the end of the PP matrix decomposition. A careful examination of the curves reveals that increasing the concentration of TPS in the composites causes weight loss to begin earlier. The second feature is that the TG curves of all composites show a plateau at the end of the experiment, indicating the presence of a carbonized PP residue.

The DTA curves show that for TPS alone, there is an endothermic peak at 100 °C, which is most likely due to the earlier material decomposition.

The second peak at 250 °C corresponds to the inflection point of the TG curve. The pic at 300 °C corresponds exactly to the starting point of the slowing down of the TG curve.

The inflection point of the TG curve is represented by the second peak at 250 °C. The image at 300 °C corresponds exactly to the beginning of the slowing of the TG curve.

The DTA curves for the remaining six composites show two endothermic peaks. The first appears around 160 °C for all formulations, while the second appears around 430 °C for (S1, S3, S4, S5) and rises to 460 °C for (S2 and S6). The peak at 160 °C corresponds to the melting temperature of PP; its glass transition temperature is typically around -25 °C, which is significantly lower than the temperature range of the test. The peak at 430°C, on the other hand, could correspond to the inflection point of the TG curve of the material decomposition. If this is true, the addition of TPS to PP (in the case of S2 and S6), with a peak temperature of 460 °C, has most likely delayed the decomposition of the composite, slightly improving its degradation temperature. According to many authors, the concentration of the other components in composite materials can affect the thermal behavior of PP, which can either improve or decrease its thermal stability [19, 35, 36].

Although there does not appear to be a well-defined tendency of increasing TPS concentration on the thermal properties of the composites in this case, the results obtained showed that the addition of TPS, a biopolymer with lower thermal properties than PP, slightly improved the thermal properties of the (PP/TPS/PP-g-MA).

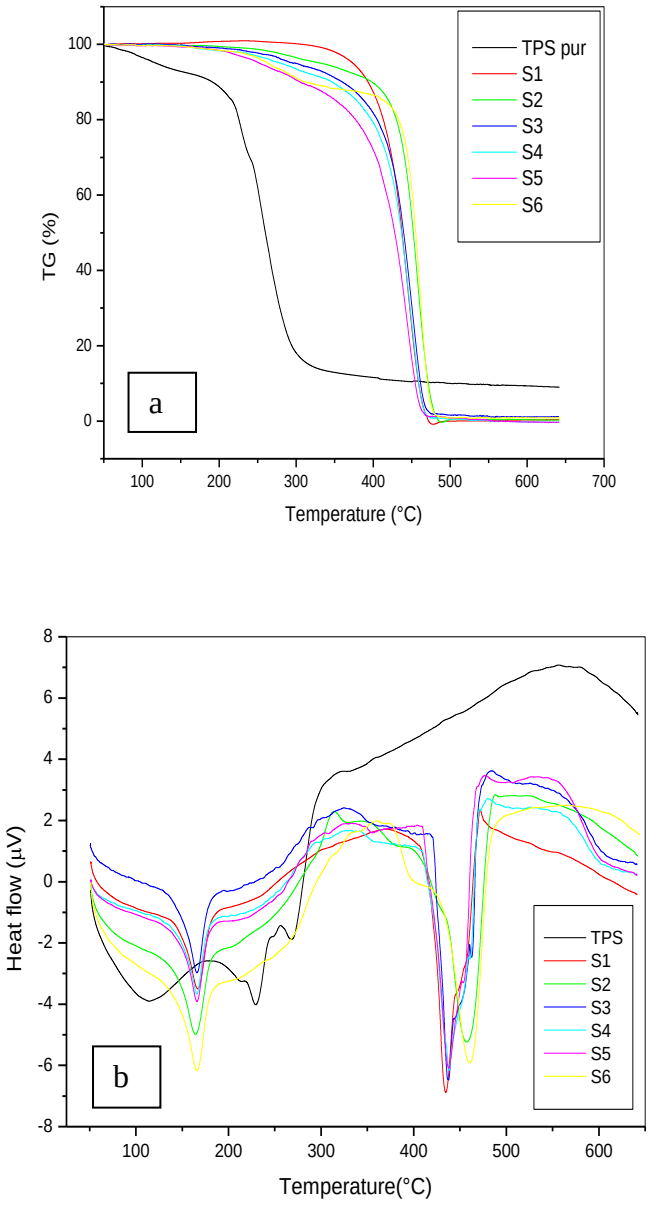

Fig. 9. TGA (a) and DTA (b) curves of TPS and PP/TPS /filler composites.

Conclusion

PP/TPS materials with a low environmental impact have been developed. Alfa (Stipa tenacissima) fibers were examined using scanning electron microscopy to determine how the alkaline treatment affected the surface appearance of the fibers before and after they were used as natural vegetal filler. The compatibilizer (PP-g-MA) has helped distribute the fiber throughout the matrix. In fact, the maleic anhydride helps to form sturdy ester bonds between the PP chain and the O-H groups of the fibers. In addition, it has been discovered that the compatibilizer's maleic anhydride functional groups, which have been grafted onto the PP (PP-g-MA), form covalent bonds with the hydrophilic starch, thereby increasing the product stability.

The stress, elongation at break, and Young's modulus are all decreased when TPS is added to PP at increasing concentrations. Although effective plasticization of starch accounts for the observed decrease in Young's modulus, these results are inconsistent with those of other research efforts. According to the results of the thermal analysis, the incorporation of TPS into the composites can either hasten or postpone the onset of thermal decomposition. Based on the results of this research, it appears that adding 15% TPS to the composite (PP/TPS/PP-g-MA/fiber) improves the interfacial cohesion and mechanical properties. Using such a composite could pave the way toward producing environmentally friendly plastics. However, more research into optimizing fiber treatment to enhance matrix/filler adhesion is encouraged. In order to achieve a completely natural composite, this study will steadily increase the concentrations of biopolymer and vegetable fibers to finally get a 100% natural composite.

References

[1] X. Ren: J. of Clean Product, 11 (2003) 27–40.
[2] Y.Kim, Y. Cheol, J. Kim, J.Chul: J Ind Eng Chem, 13 (2007) 1029-1034.
[3] I.Varyan, N. Kolesnikova, H. Xu, P.Tyubaeva, A. Popov: Effect of Natural Rubber Polym, 14 (2022) 1-19.
[4] A. A. Popov: Polym Sci, A, 63 (2021) 623-636.
[5] J. H. Sung, D. P. Park, B. J. Park, H. J. Choi: J Ind Eng Chem, 12 (2006) 301-305.
[6] M. Barikani, M. Mohammadi: Carbohydr Polym, 68 (2007) 773-780.
[7] S. Momeni, E.R. Ghomi, M. Shakiba, S.S.Navid, M. Abdouss, A. Bigham, F. Khosravi, Z. Ahmadi, M. Faraji, H. Abdouss, S. Ramakrishna: Polym, 13 (2021) 1-19.
[8] R.Tessier, E. Lafranche, P. Krawczak: Express Polym Lett, 6 (2012) 937-952.
[9] J.M. Millican, S. Agarwal: Macromolecules, 54 (2021) 4455-4469.
[10] K.E.R. Velasco, C.A.U. Silva, A.D. Barrios, A.E.S. Márquez, J. P. Tafur, R. M. Michell: Polym Rev, 13 (2021) 1-36.
[11] B. Khan, M. Bilal, K. Niazi, G. Samin, Z.Jahan : J. of Food Proc. Eng, 40 (2017) 1-17.
[12] Z.N. Diyana, R. Jumaidin, M.Z. Selamat, I. Ghazali, N. Julmohammad, N. Huda, R.A. Ilyas: Polymers, 13 (2021) 1-20.
[13] S. Tabasum, M. Younas, M.A. Zaeem, I. Majeed, M. Majeed, A. Noreen, M.N. Iqbal, K. M. Zia: Int J Biol Macromol, 1 (2019) 969-996.
[14] L. Ribba, M.C. Lorenzo, M. Tupa, M. Melaj. P. Eisenberg, S. Goyanes, Green Composites, First ed., Springer, Singapore 2021, 63-133.
[15] H. Wu, A. Hou, X. Hu, X. Lu, J.P. Qu: Ind Crops Prod, 176 (2022) 114-323.

[16] M.M. Marvizadeh, A. Tajik, V. Moosavian, N. Oladzadabbasabadi, A.M. Nafchi: J Chem Health Risks, 11 (2021) 23-29.
[17] N. Mohammadi, A.M. Moradpour, M. Saeidi, A.K. Alias: Starch Stärke, 65 (2013) 61–72.
[18] A.S. Abreu, M. Oliveira, A.V. Machado: Appl Clay Sci, 104 (2015) 277–285.
[19] E. Raee, B. Kaffashi: J Appl Polym Sci, 135 (2018) 45740.
[20] N. Toumi, M. Guessoum, S. Nekkaa, J. of Adh Sci Tech. 33 (2019) 2071–2092.
[21] E. Manias, A. Touny, L. Wu, K. Strawhecker, B. Lu, T.C. Chung: Chem Mater, 13 (2001) 3516-3523.
[22] A. B. Linares, J. C. Jiméneza, P. Lópezb, B. Rojas de Gáscu: Orbital – Electro J Chem, 11 (2019), 71-82.
[23] I.M. Thakore, S. Desai, B.D. Sarawade, S. Devi: Eur polym J, 37 (2001) 151-160.
[24] K. E. Borchani, C. Carrot, Mohamed Jaziri: Composites Part A: Appl Sci Manuf, 78 (2015) 371-379.
[25] M. Rokbi, H. Osmani, A. Imad, N. Benseddiq: Procedia Eng, 10 (2011) 2092-2097.
[26] S. Ajouguim, K. Abdelouahdi, M. Waqif, M. Stefanidou, L. Saâdi: Cellulose, 26 (2019) 1503–1516.
[27] G.S. Bajwa, R.M. Singari, R.S. Mishra: Indian J Pure Appl Phys, 59 (2021) 372-378.
[28] W. Liu, Y.-J. Wang, Z. Sun, J Appl Polym Sci, 88 (2003) 2904–2911
[29] J.F. Mendes, R.T Paschoalin, V.B.C. Alfredo, R.S. Neto, A.C.P. Marques, J.M. Marconcini, L.H.C. Mattoso, E.S. Medeiros, J.E. Oliveira: Carbohydrate Polym, 137 (2016) 452-458.
[30] F. Hafidzah, M. Bijarimi, W. Alhadadi, S. Salleh, M. Norazmi, E. Normaya: Indonesian J Chem, 21 (2021) 234-242.
[31] M. Kaseem, K. Hamad, F. Deri: Polym Bull 68 (2012) 1079-1091.
[32] S. Hanifi, A. Oromiehie, S. Ahmadi, H. Farhadnejad: J Vinyl Addit Technol, 20 (2014) 16-23.
[33] L. A. Castillo, O. V. Lopez, M. A. García, S. E. Barbosa, M. A. Villar: Heliyon, 5 (2019) e01877.
[34] [34] F.J. Rodriguez-Gonzalez, B.A. Ramsay, B.D. Favis: Polymer, 44 (2003) 1517–1526.
[35] J. Gersten, V. Fainberg, G. Hetsroni, Y. Shindler: Fuel, 79 (2000) 1679–1686
[36] M. S. Mat-Shayuti, M. Z. Abdullah, P. S. M. Megat-Yusoff: MATEC Web of Conferences 69, 03001 (2016).